

High-Spin Diimine Complexes of Iron(II) Reject Binding of Carbon Monoxide: Theoretical Analysis of Thermodynamic Factors Inhibiting or Favoring Spin-Crossover

Ned J. Hardman, Xinggao Fang, Brian L. Scott, Robert J. Wright, Richard L. Martin,* and Gregory J. Kubas*

Chemistry Division and Theoretical Division, Los Alamos National Laboratory, MS-J514, Los Alamos, New Mexico 87545

Received June 14, 2005

A new series of Fe(II) complexes, $\text{FeCl}_2\{\text{N}(\text{R})=\text{C}(\text{Me})\text{C}(\text{Me})=\text{N}(\text{R})\}$, containing diimine ligands with hemilabile sidearms R (R = $\text{CH}_2(\text{CH}_2)_2\text{NMe}_2$, **1**, $\text{CH}_2(\text{CH}_2)_2\text{OMe}$, **2**, $\text{CH}_2(\text{CH}_2)_2\text{SMe}$, **3**) were synthesized. The crystal structure of **1** showed 6-coordination where both amine arms were attached, whereas **2** was a 5-coordinate 16e species with one methoxy arm dangling free. Extensive attempts were made to bind CO to these species to synthesize precursors for dihydrogen complexes but were unsuccessful. Reaction of **1** with 1 or 2 equiv of AgOTf under CO atmosphere resulted in isolation of only a 6-coordinate bis(triflate)-containing product $[\text{Fe}\{\text{N}(\text{R})=\text{C}(\text{Me})\text{C}(\text{Me})=\text{N}(\text{R})\}(\text{OTf})_2]$ (R = $\text{CH}_2(\text{CH}_2)_2\text{NMe}_2$), **5**. Reaction of 5-coordinate **2** with AgSbF_6 under CO did not give a CO adduct but afforded instead a dicationic dinuclear complex $[\text{Fe}\{\text{N}(\text{R})=\text{C}(\text{Me})\text{C}(\text{Me})=\text{N}(\text{R})\}(\mu\text{-Cl})_2][\text{SbF}_6]_2$ (R = $\text{CH}_2(\text{CH}_2)_2\text{OMe}$), **4**, containing a weakly bound SbF_6 . Thus coordination of hard-donor anions to iron was favored over CO binding. The unexpected rejection of binding of CO is rationalized by the iron being in a high-spin state in this system and energetically incapable of spin crossover to a low-spin state. Theoretical calculations on CO interaction with Fe(II) centers in spin states $S = 0, 1$, and 2 for both the 16e complexes and their CO adducts aid further understanding of this problem. They show that interaction of CO with a high-spin 5-coordinate Fe model diimine complex is essentially thermoneutral but is exergonic by about 48 kcal/mol to a comparable but low-spin diposphine fragment. Spin crossover is thus disfavored thermodynamically rather than kinetically (e.g. a “spin block” effect); i.e., the ligand field strengths of the primarily N-donor groups are apparently insufficient to give a low-spin CO adduct.

Introduction

Knowledge about the bonding and coordination properties of transition metal fragments and ligands is often most easily gained by observing the strength of interaction of specific ligands with specific metal centers in various oxidation and spin states. Occasionally there are surprises, as exemplified by the ability of metal complexes to coordinate closed-shell molecules (and thus seemingly weak ligands) such as molecular hydrogen¹ and alkanes^{1,2} and even noble gases such as xenon.³ In the reverse sense it is noteworthy when coordinatively unsaturated complexes reject binding of powerful ligands such as CO, which has been characterized to be a “universal ligand” to lower valent metal centers.⁴

Strong CO binding to iron in hemoglobin is particularly notorious in regard to the toxicity of CO. Of particular relevance in Fe–heme systems is the spin-state change (spin crossover) from high-spin Fe^{II} ($S = 2$) to low-spin Fe^{II} ($S = 0$) on CO binding,⁵ which are much less facile in inorganic and organometallic complexes than may generally be appreciated. Anomalously weak CO binding in $\text{Cp}_2\text{VI}(\text{CO})$ and $\text{Cp}_2\text{Cr}(\text{CO})$ was noted decades ago independently by Calder-

* To whom correspondence should be addressed. E-mail: kugas@lanl.gov (G.J.K.); rlmartin@lanl.gov (R.L.M.).

(1) *Metal Dihydrogen and σ -Bond Complexes*; Kubas, G. J., Kluwer Academic/Plenum Publishers: New York, 2001.

(2) (a) Hall, C.; Perutz, R. N. *Chem. Rev.* **1996**, *96*, 3125. (b) Geftakis, S.; Ball, G. E. *J. Am. Chem. Soc.* **1998**, *120*, 9953. (c) Evans, D. R.; Drovetskaya, T.; Bau, R.; Reed, C. A.; Boyd, P. D. W. *J. Am. Chem. Soc.* **1997**, *119*, 3633. (d) Castro-Rodriguez, I.; Nakai, H.; Gantzel, P.; Zakharov, L. Z.; Rheingold, A. L.; Meyer, K. *J. Am. Chem. Soc.* **2003**, *125*, 15734.

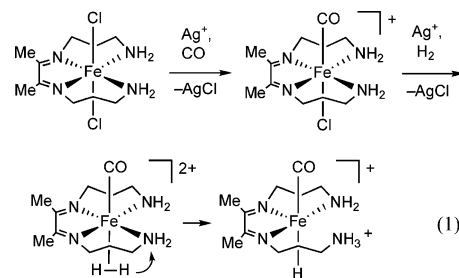
(3) (a) Seidel, S.; Seppelt, K. *Science* **2000**, *290*, 117. (b) Ball, G. E.; Darwish, T. A.; Geftakis, S.; George, M. W.; Lawes, D. J.; Portius, P.; Rourke, J. P. *Proc. Natl. Acad. Sci. U.S.A.* **2005**, *102*, 1853.

(4) Radius, U.; Bickelhaupt, F. M.; Ehlers, A. W.; Goldberg, N.; Hoffmann, R. *Inorg. Chem.* **1998**, *37*, 1080.

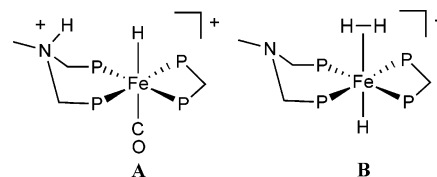
azzo and Brintzinger, both of whom rationalized that spin pairing has to take place upon carbonylation of the high-spin fragments.⁶ In his review article on such effects of spin state, Poli^{6c} notes that “despite this early work, the importance of electron pairing in organometallic stability and reactivity has remained essentially unappreciated.” This was certainly the case in our comprehension of the results of the work that will be described below.

Recent interest in iron–carbonyl systems has increased due to the discovery of the Fe–CO motif in the novel organometallic-like active site of hydrogenase metalloenzymes, the first time CO (and cyanide) coordination has been observed in Nature.^{7,8} Hydrogenases are an area of intense current interest in regard to modeling both their structure and function, especially for purposes of biomimetic hydrogen production.^{7c,d,f,8,9} The spin state of iron, which is always *low spin* in all redox states of hydrogenases, is of critical importance in maintaining the necessary strong binding of CO to Fe in hydrogenases. In accord with the general principles of transition metal chemistry,^{5d,6c} the overall ligand field strength strongly influences the spin state of the dimetallic active sites, which generally feature Fe(CO)(CN) moieties linked by thiolate bridges. As will be shown, this must be taken into account in efforts to model any facet of hydrogenase chemistry. In particular, we desired to use organometallic metal centers to model the enzyme’s remarkably facile ability to both heterolytically cleave H₂ and form H₂ from protons and electrons. This type of reactivity as well as reversible binding/release of molecular H₂ (versus hydride) is favored on inorganic complexes by the presence of CO ligands (particularly when trans to bound H₂), which may explain the unique occurrence of CO in hydrogenases.^{1,7d}

We thus intended to synthesize Fe^{II} complexes with CO trans to H₂ to observe *intramolecular* heterolysis of H₂ where a proton transfers to a basic cis ligand, e.g. via eq 1:



Similarity to the active site of hydrogenase (which is totally different) was not of concern, and we had previously studied the multidentate α -diimine ligands in eq 1 on Pd^{II} and Pt^{II} centers.¹⁰ The important feature is that the diimines contain basic pendant sidearms (the amine groups in eq 1) that could accept a proton from H₂ heterolysis. Pd–diimine complexes bind silanes as σ ligands and heterolyze their η^2 -Si–H bonds, although via a different pathway. Intramolecular heterolysis of η^2 -H₂ on Fe^{II} centers as in eq 1 had not been previously directly observed, although while our work was in progress DuBois¹¹ independently looked for such heterolysis in a related phosphine system, *trans*-[Fe(X)(Y)(PNP)(dmpm)]⁺, also containing a proximal basic amine group. Protonation of [FeH(CO)(PNP)(dmpm)]⁺ was observed to occur at the N atom of the PNP ligand to form **A** rather than at the hydride ligand to give a dihydrogen complex, implying that if an incipient H₂ ligand formed, it would be more acidic



than the protonated PNP⁺ ligand. However when a hydride is positioned trans, instead of CO, H₂ binds but does not heterolyze to protonate the amine (**B**). Thus, heterolysis of η^2 -H₂ is much more effective when CO is trans to it because the η^2 -H₂ becomes more acidic due to electron removal by the strongly π accepting CO.

In our anticipated scheme (eq 1), stepwise removal of chloride ligands from a dichloro precursor using Ag⁺ would have been expected to produce a complex with H₂ trans to CO, and the acidic H₂ ligand might then protonate the cis pendant amine. However, the very first step unexpectedly proved to be a major barrier: the metal–diimine system rejected binding of CO, as will be discussed below. The apparent rationale for this is that the iron is in a high-spin state in the Fe(diimine)Cl₂ precursor and [Fe(diimine)Cl]⁺ fragments formed on Cl abstraction and does not undergo spin crossover to a low-spin state that would appear to be necessary for stable CO binding. However, DuBois had found that the precursor to complexes **A** and **B** above, *trans*-FeCl₂-(PNP)(dmpm), is also paramagnetic but does directly react

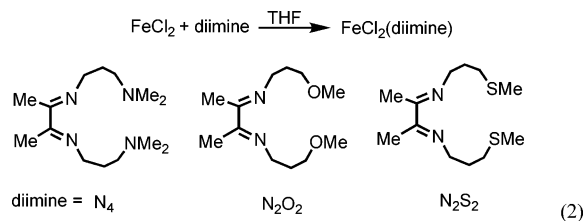
- (5) (a) Alberding, N.; et al. *Biophys. J.* **1978**, *24*, 319. (b) McMahon, B. H.; Stojkovic, B. P.; Hay, P. J.; Martin, R. L.; Garcia, A. E. *J. Chem. Phys.* **2000**, *113*, 6831. (c) Thompson, D. W.; Kretzer, R. M.; Lebeau, E. L.; Scaltrito, D. V.; Ghilardi, R. A.; Lam, K.-C.; Rheingold, A. L.; Karlin, K. D.; Meyer, G. J. *Inorg. Chem.* **2003**, *42*, 5211. (d) *Spin Crossover in Transition Metal Compounds I*; Topics in Current Chemistry 235; Gütllich, P., Goodwin, H. A., Eds.; Springer-Verlag: Berlin, Heidelberg, Germany, 2004. (e) Harvey, J. N. *J. Am. Chem. Soc.* **2000**, *122*, 12401.
- (6) (a) Calderazzo, F.; Fachinetti, G.; Floriani, C. *J. Am. Chem. Soc.* **1974**, *96*, 3695. (b) Wong, K. L. T.; Brintzinger, H. H. *J. Am. Chem. Soc.* **1975**, *97*, 5143. See also: (c) Poli, R. *Chem. Rev.* **1996**, *96*, 2135. (d) Poli, R. *J. Organomet. Chem.* **2004**, *689*, 4291.
- (7) (a) Peters, J. W.; Lanzilotta, W. N.; Lemon, B. J.; Seefeldt, L. C. *Science* **1998**, *282*, 1853. (b) Nicolet, Y.; Piras, C.; Legrand, P.; Hatchikian, C. E.; Fontecilla-Camps, J. C. *Structure* **1999**, *7*, 13. (c) Darensbourg, M. Y.; Lyon, E. J.; Smece, J. J. *Coord. Chem. Rev.* **2000**, *206–207*, 533. (d) Huhmann-Vincent, J.; Scott, B. L.; Kubas, G. J. *Inorg. Chim. Acta* **1999**, *294*, 240. (e) Niu, S.; Thomson, L. M.; Hall, M. B. *J. Am. Chem. Soc.* **1999**, *121*, 4000. (f) Armstrong, F. A. *Curr. Opin. Chem. Biol.* **2004**, *8*, 133. (g) Volbeda, A.; Fontecilla-Camps, J. C. *Dalton Trans.* **2003**, 4030. (h) Reissmann, S.; Hochleitner, E.; Wang, H.; Paschos, A.; Lottspeich, F.; Glass, R. S.; Bock, A. *Science* **2003**, *299*, 1067.
- (8) (a) Tard, C.; Liu, X.; Ibrahim, S. K.; Bruschi, M.; De Gioia, L.; Davies, S. C.; Yang, X.; Wang, L.-S.; Sawers, G.; Pickett, C. J. *Nature* **2005**, *433*, 610. (b) Evans, D. J.; Pickett, C. J. *Chem. Soc. Rev.* **2003**, *32*, 268.
- (9) (a) Jiang, J.; Koch, S. A. *Inorg. Chem.* **2002**, *41*, 158. (b) Kayal, A.; Rauchfuss, T. B. *Inorg. Chem.* **2003**, *42*, 5046.

- (10) (a) Fang, X.; Scott, B. L.; Watkin, J. G.; Kubas, G. J.; *Organometallics* **2000**, *19*, 4193. (b) Fang, X.; Watkin, J. G.; Scott, B. L.; Kubas, G. J. *Organometallics* **2001**, *20*, 3351.
- (11) Henry, R. M.; Shoemaker, R. K.; Newell, R. H.; Jacobsen, G. M.; DuBois, D. L.; Rakowski DuBois, M. *Organometallics* **2005**, *24*, 2481.

with CO to displace chloride to form diamagnetic $[trans\text{-Fe}(\text{PNP})(\text{dmpm})\text{Cl}(\text{CO})]^+$, a rare example of spin crossover. So why the difference? The inability of our and most Fe^{II} high-spin systems to undergo carbonylation was initially considered by us to possibly be symptomatic of a “spin-blocked” reaction, where a barrier may exist due to the crossing between reactant quintet and product singlet surfaces.¹² Whether spin-state changes inhibit organometallic reactions has been a decades-old debate and has recently been shown computationally by Harvey and Poli to be highly dependent on the system.¹² However, this and other current literature indicate that the term “spin-block” (or “spin-forbidden”) should be reserved for kinetic effects, and as will be shown, theoretical calculations on CO interaction with model Fe^{II} -diimine centers demonstrates that the lack of CO binding is thermodynamic in origin. Thus, in our system versus the phosphine system, ligand field strength of the N-donor versus P-donor ligands is of critical importance. However a priori prediction of whether placement of diphosphine versus diimine donors on iron gives more electron-rich centers that favor carbonylation is not clear from first principles. Our work shows that theoretical DFT calculations can give some guidance to whether this or other similar problematic ligand additions are spin forbidden processes or just weak ligand field issues.

Results

The complexes $(\text{N}_4)\text{FeCl}_2$ (**1**), $(\text{N}_2\text{O}_2)\text{FeCl}_2$ (**2**), and $(\text{N}_2\text{S}_2)\text{FeCl}_2$ (**3**) were readily prepared by reaction of FeCl_2 with diimine ligands¹¹ with pendant hemilabile sidearms (eq 2).



NMR spectroscopy indicated that deep blue **1–3** (and related complexes discussed below) were paramagnetic with $\mu_{\text{eff}} = 4.75\text{--}5.03 \mu_{\text{B}}$ (Bohr magnetons (BM)) as determined through the use of Evan’s method. This is consistent with the presence of four unpaired electrons for which a value of $4.90 \mu_{\text{B}}$ would be expected. An X-ray crystal structure of **1** showed octahedral geometry with attachment of both arms and a cis arrangement of chlorides (Figure 1). On the other hand, the analogous complex **2** with pendant methoxy groups possessed a 5-coordinate square pyramidal structure with a dangling methoxy (Figure 2). The distances from iron to the imine nitrogen atoms in **1**, **2**, and the two related complexes **4** and **5** discussed below average 2.162 \AA (Table 1). In comparison, low-spin diimine octahedral complexes show significantly shorter M–N bond lengths (ca. 1.9 \AA). The bond lengthening is consistent with assignment of these species as high-spin octahedral complexes with four unpaired electrons.

(12) (a) Carreon-Macedo, J.-L.; Harvey, J. N. *J. Am. Chem. Soc.* **2004**, *126*, 5789. (b) Poli, R. N.; Harvey, J. N. *Chem. Soc. Rev.* **2003**, *32*, 1.

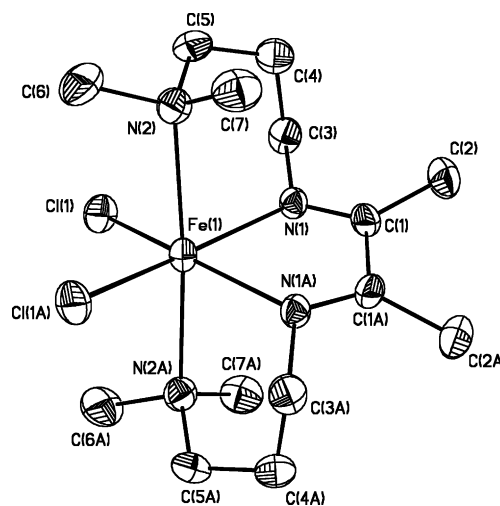


Figure 1. X-ray crystal structure of $(\text{N}_4)\text{FeCl}_2$ (**1**).

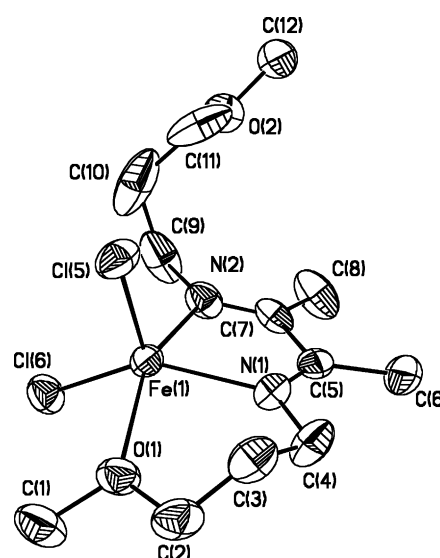


Figure 2. X-ray crystal structure of $(\text{N}_2\text{O}_2)\text{FeCl}_2$ (**2**).

Table 1. Selected Bond Distances (\AA) and Angles (deg) for Diimine Complexes

complex	Fe–Cl	Fe–N _{imine}	Fe–N _{amine}	Fe–O ^a
1 , $(\text{N}_4)\text{FeCl}_2$	2.399(1)	2.177(3)	2.411(3)	
2 , $(\text{N}_2\text{O}_2)\text{FeCl}_2$	2.314(1)	2.143(3)		2.228(3)
4 , $(\text{N}_4)\text{Fe}(\text{OTf})_2$		2.222(6)	2.306(6)	2.121(4)
5	2.424(2)	2.105(7)		2.114(6)

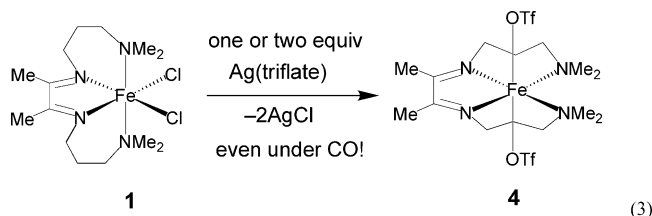
^a O = methoxy or triflate oxygen.

The strategy according to eq 1 was to initially directly replace one Cl with CO either as in the synthesis of $[\text{Fe}(\text{depe})_2(\text{CO})(\text{Cl})][\text{Cl}]$ (depe = $\text{Et}_2\text{PC}_2\text{H}_4\text{PET}_2$) originally reported by Bellerby and co-workers¹³ or if need be with the help of silver salts to abstract the Cl. Bellerby was able to form the CO complex in methanol solution by displacement of one chloride from $[\text{Fe}(\text{depe})_2(\text{Cl})_2]$ to an outer sphere location (i.e. anion) by 1 equiv of CO.^{13a} However, in our system, Cl^- was not displaced by CO from complexes **1–3** in methanol, tetrahydrofuran, or toluene solvents. Removal

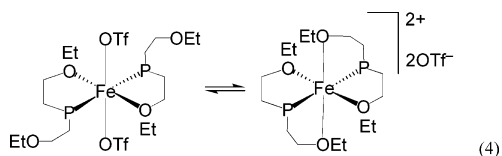
(13) (a) Bellerby, J. M.; Mays, M. J.; Sears, P. L. *J. Chem. Soc., Dalton Trans.* **1976**, 1232. (b) Landau, S. E.; Morris, R. H.; Lough, A. J. *Inorg. Chem.* **1999**, *38*, 6060.

High-Spin Diimine Complexes of Iron(II)

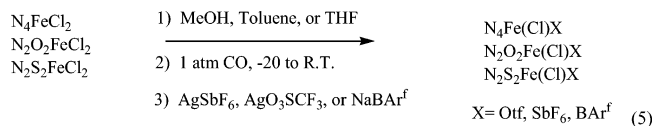
of chloride from the complex was then forced by adding equimolar amounts of AgOTf, AgSbF₆, or NaBar^f to the CO-saturated solutions described above. Reactions of the iron diimine complexes with silver salts readily occurred to give partial or complete chloride removal. However, regardless of the presence or absence of CO, the sought after synthesis of [(N₄)Fe(CO)(Cl)][OTf] resulted instead in the isolation of (N₄)Fe(OTf)₂ (**4**) containing coordinated triflate (eq 3).



Following the same general procedures listed above and even when 0.8 equiv of AgOTf was used, the only isolated product was purple crystalline **4** in poor yields (10–15%). A high-yield synthesis of **4** was devised by reacting 2 equiv of AgOTf with (N₄)FeCl₂ in toluene at 0 °C. The X-ray structure of **4** (Figure 3) shows that the N₄ ligand is flexible and has rearranged position to lie in a plane, which had been the desired stereochemistry in eq 1. However the trans triflate ligands were relatively tightly bound and could not be displaced by CO. **4** is paramagnetic and can be compared to a complex with trans triflates and hemilabile ether phosphine ligands prepared similarly and characterized crystallographically (eq 4).¹⁴ In contrast, this complex is low-spin diamagnetic, and in nitromethane the triflates dissociate and the pendant ethoxy groups coordinate (eq 4).



A series of reactions (eq 5) according to the same general method as for the preparation of **4** in eq 3 were carried out in an attempt to prepare species of the type [N₄Fe(Cl)(X)], [N₂O₂Fe(Cl)(X)], and [N₂S₂Fe(Cl)(X)] (X = OTf, SbF₆, BAR^f). Although the products were not as tractable as **4**, they displayed paramagnetic behavior in the NMR and no IR bands above 1750 cm⁻¹ that would be diagnostic of CO coordination. This was especially surprising in the case of 5-coordinate (N₂O₂)FeCl₂ which might have been expected to simply add CO as a sixth ligand even without chloride removal. As there are no known examples of high-spin octahedral Fe–CO complexes, it was assumed that the only reaction that occurred here was anion exchange.



Since the triflate anion was too strongly coordinating in **4**, it was decided to more carefully investigate chloride

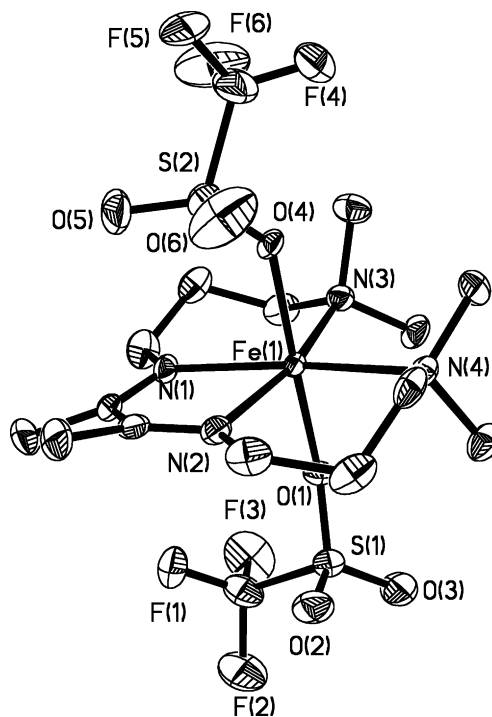
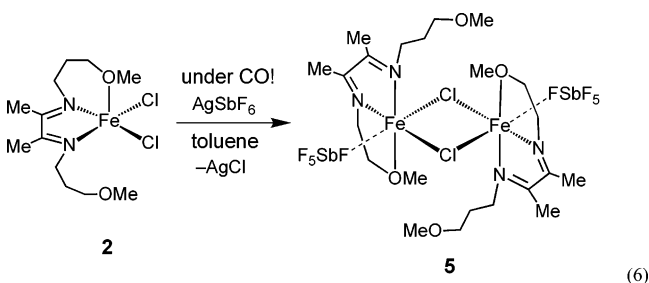


Figure 3. X-ray crystal structure of N₄Fe(OTf)₂ (**4**). Hydrogen atoms have been omitted for clarity.

removal under an atmosphere of CO using AgSbF₆ with a low coordinating anion. As a further incentive for CO to bind to Fe, the five-coordinate complex (N₂O₂)FeCl₂ was employed as the precursor. Surprisingly, a chloride-bridged complex, **5**, resulted, wherein the metal centers are weakly interacting with the SbF₆ anions at the sixth coordination site rather than binding CO or even the dangling methoxy groups (eq 6).



The X-ray structure of **5** showed that the distance from iron to the fluorine in the SbF₆ groups (2.448(8) Å) was much longer than that observed¹⁵ in Fe^{III}(TPP)(FSbF₅) (TPP = tetraphenylporphyrinato), 2.105(3) Å, indicating the interaction is weak (Figures 4 and 5). The Fe–F length is also much longer than in low-spin [Fe^{II}(FBF₃)(CO)(depe)]⁺ (2.081(6) Å), which contains BF₄ coordinated trans to CO.^{13b} The distance is comparable to that in high-spin 5-coordinate Fe^{II}-(py)(NRAr_F)₂ (Ar_F = 2,5-C₆H₃FMe) which features distances of 2.447(2) and 2.378(2) Å between the iron and aryl fluorine

(14) Chadwell, S. J.; Coles, S. J.; Edwards, P. G.; Hursthouse, M. B. *J. Chem. Soc., Dalton Trans.* **1996**, 1105.

(15) Shelly, K.; Bartczak, T.; Scheidt, W. R.; Reed, C. A. *Inorg. Chem.* **1985**, *24*, 4325.

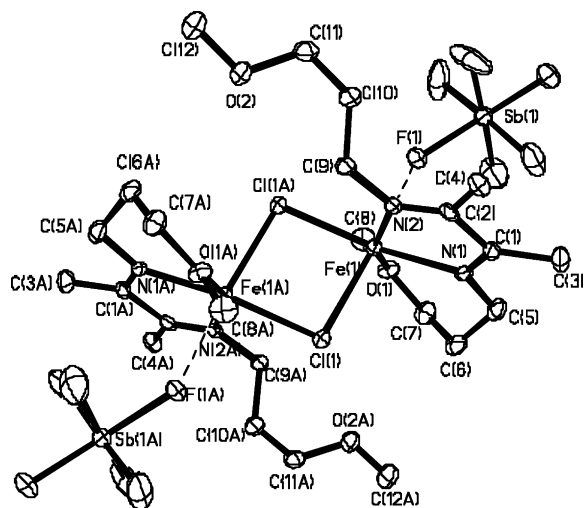


Figure 4. X-ray crystal structure of $[(\eta^3\text{-N}_2\text{O}_2)\text{Fe}(\mu\text{-Cl})(\text{SbF}_6)]_2$ (**5**). Hydrogen atoms have been omitted for clarity.

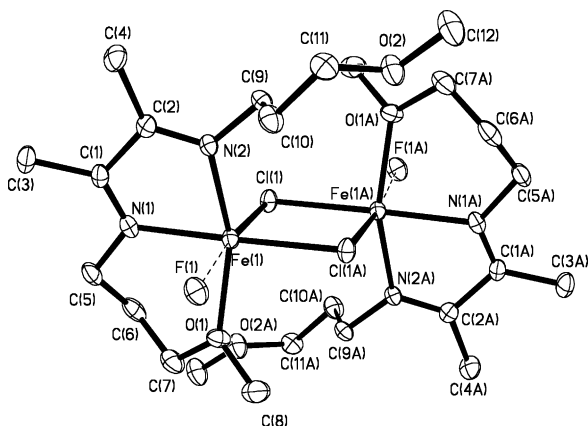


Figure 5. X-ray crystal structure of **5** (another view). Hydrogen atoms and both SbF_6 groups connected to F(1) and F(1A) have been omitted for clarity.

atoms in the bidentate N,F-donor chelates.¹⁶ The bond angles in **5** are $88.2(2)^\circ$ (Cl–Fe–F), $85.8(2)^\circ$ (N1–Fe–F), and $84.4(5)^\circ$ (N2–Fe–F) indicating a roughly octahedral geometry in the solid state. In solution, Evan's method yielded a value of $4.84 \mu_B$ for **5** (for a mononuclear formula unit), indicating it has four unpaired electrons.

Theoretical Calculations

To help rationalize the rejection of CO binding, DFT calculations were undertaken on model $[(\text{N}_4)\text{FeCl}]^+$ fragments and their CO adducts in singlet, triplet, and quintet states. Also a similar diphosphine system was analyzed to compare its binding energy to CO. We investigated the electronic structure of these species with hybrid density functional theory (B3LYP).¹⁷ The calculations utilized the 6-31G* basis set for the ligand atoms and Wachter's-based 6-311+g for the metal. The ground state of the model complex $[\text{trans}-(\text{N}_4)\text{FeCl}(\text{CO})]^+$ is calculated to be a spin singlet

(16) Stokes, S. L.; Davis, W. M.; Odom, A. L.; Cummins, C. C. *Organometallics* **1996**, *15*, 4521.

(17) The calculations utilized the Gaussian03 suite of electronic structure codes: Frisch, M. J.; et al. *Gaussian03*; Gaussian, Inc.: Wallingford, CT, 2004.

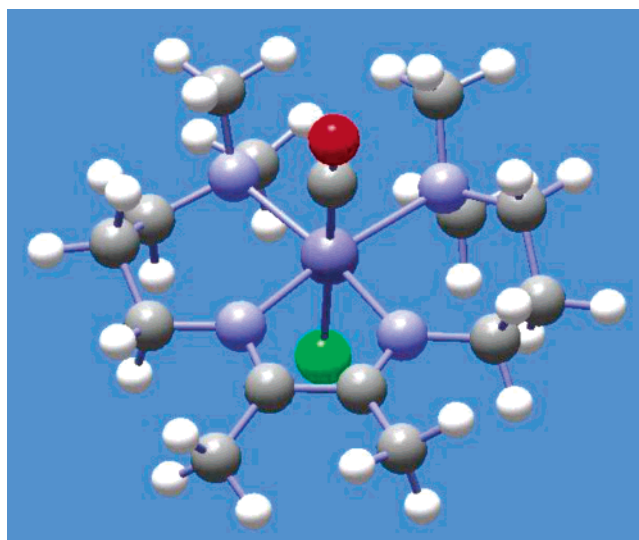


Figure 6. Calculated structure of the CO adduct of the FeN_4Cl fragment.

($S = 0$) (Figure 6, Table 2). Because of the difficulties in actual synthesis of this complex, we investigated whether the carbonyl adduct is bound with respect to a five-coordinate cationic complex $[(\text{N}_4)\text{FeCl}]^+$ and a free CO. The optimum geometry for the five-coordinate singlet species is a very slightly distorted square pyramid (Figure 7, Table 2). All the Fe–N distances are somewhat shorter than in the carbonyl adduct. Relative to this fragment, the CO is bound by 30.8 kcal/mol in the adduct. In contrast, the quintet state of the $[(\text{N}_4)\text{FeCl}]^+$ fragment is significantly lower in energy than the singlet, and the singlet–quintet energy difference (with each species at its optimum geometry) is 32.1 kcal/mol. The reaction of CO with the high-spin fragment (and attendant spin crossover) is therefore predicted to be essentially *thermoneutral*; i.e., the 5-coordinate 16e complex is slightly favored and the binding of CO is endergonic by ~ 1 kcal/mol. Obviously CO binding is additionally disfavored entropically, and thus, ΔG would be significantly endothermic, in accord with the experimental observation that CO does not coordinate. The energies for the $S = 1$ states for both the fragment and the CO adduct were calculated also and are compared to the results for the singlet and quintet states in Table 3. For the 16e fragment, the triplet state lies nearly halfway between the singlet and quintet states (18.3 kcal/mol above the singlet even in their optimized geometries), and thus, a so-called “intermediate spin” 5-coordinate Fe^{II} species^{5c} is not likely to have relevance here.

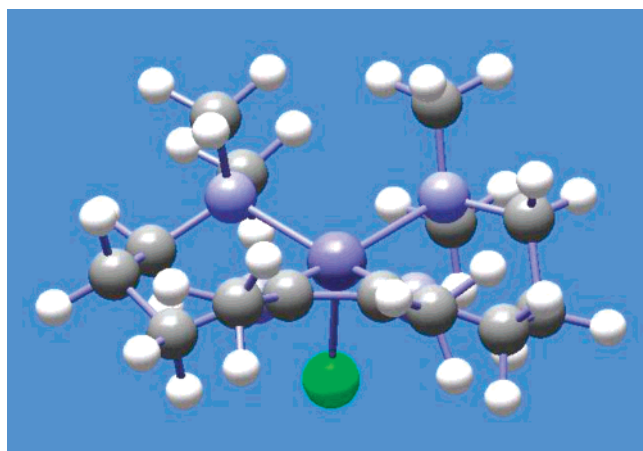
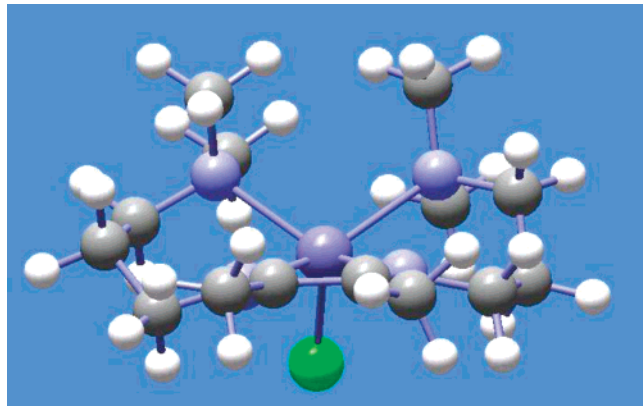
There are considerable differences in the geometries of the 16e fragments in their optimized, relaxed states versus the fixed geometry of the complex in the quintet state, as reflected also by the energy differences (Table 3). Relative to the singlet, the quintet fragment is more puckered, and the Fe–N distances are longer, as would be expected (Figure 8, Table 2). The calculated Fe–N_{imine} distance ($\sim 2.20 \text{ \AA}$) for cationic $[(\text{N}_4)\text{FeCl}]^+$ is slightly greater than the experimental distance for the neutral complex $(\text{N}_4)\text{FeCl}_2$ (2.177 \AA , Table 1). The corresponding bond length for the singlet fragment ($\sim 2.00 \text{ \AA}$) is significantly shorter than the experimental value. Another interesting feature of the calculations

Table 2. Calculated Bond Distances (Å) and Angles (deg) for Model Complexes in Figures 6–8

complex	Fe–Cl	Fe–N _{imine}	Fe–N _{amine}	Fe–CO	C–O	Cl–Fe–N
[(N ₄)FeCl] ⁺ , singlet	2.25	1.98, 2.01	2.24, 2.30			94–98
[(N ₄)FeCl] ⁺ , quintet	2.25	2.19, 2.20	2.35, 2.45			99–115
[(N ₄)FeCl(CO)] ⁺ , singlet	2.31	2.04, 2.05	2.31, 2.36	1.81	1.15	

Table 3. Calculated Energies (kcal/mol) for Model Complexes, Relative to Quintet States (Fragment) and the Singlet State (CO Adduct)

spin state	[(N ₄)FeCl] ⁺ ^a	[(N ₄)FeCl] ⁺ ^b	[(N ₄)FeCl(CO)] ⁺
singlet (<i>S</i> = 0)	32.1	49.6	0.0
triplet (<i>S</i> = 1)	18.3	29.2	4.5
quintet (<i>S</i> = 2)	0.0	0.0	22.2

^a Optimized geometries. ^b At the geometry of the quintet state.**Figure 7.** Calculated structure of the five-coordinate singlet FeN₄Cl fragment.**Figure 8.** Calculated structure of the five-coordinate quintet FeN₄Cl fragment.

is the unsymmetrical coordination of the amine nitrogens in the [(N₄)FeCl]⁺ model complexes, which show two distinct Fe–N_{amine} distances (Table 2). The calculations start with a nearly planar geometry, i.e., one that would result if CO dissociated from [(N₄)FeCl(CO)]⁺. What happens in the optimization is a slight pyramidalization about the Fe. A secondary effect is that one of the Me groups on the amine functionality distorts as if a C–H bond is trying to occupy the empty sixth coordination spot to form an agostic interaction. The methyl group swings away from an initial angle of about 114° (Fe–N–CH₃) to one that is around 110°, resulting in the short 2.35 Å bond. The other “equivalent” one, with the long 2.45 Å distance, maintains an angle Fe–

N–CH₃ of about 116°. The system thus seems to prefer getting one strong and one weak amine interaction with the metal versus two moderate ones.

We have also studied the analogous *diphosphine* model complex [FeCl(Me₂PC₂H₄PM₂)₂]⁺ in its known singlet state, and it is square pyramidal as for the diimine ligand system. The Cl–Fe–P angles are ~91° with but a very slight pyramidalization about Fe. Experimentally, six-coordinate neutral and cationic Fe–phosphine complexes are typically diamagnetic low-spin systems and strongly bind CO. Ruthenium analogues [RuCl(R₂PC₂H₄PR₂)₂]⁺ (R = Ph, Cy) have been structurally characterized to be genuine 16e five-coordinate complexes with geometries closer to trigonal bipyramidal.¹⁸ In the Fe–CO model complex, [FeCl(CO)-(Me₂PC₂H₄PM₂)₂]⁺, the CO is calculated to be bound much more strongly than in [(N₄)FeCl(CO)]⁺. The B3LYP calculation suggests the bond strength is 47.5 kcal/mol relative to the singlet five-coordinate fragment. Using the optimal geometry calculated for the singlet state, the high-spin fragment is calculated to lie 13 kcal/mol higher in energy. This preference for the singlet fragment in the case of the phosphine ligands is basically a consequence of the strong ligand crystal field strength here, i.e., the expected much higher energy difference between the e_g and t_{2g} orbitals.

Discussion

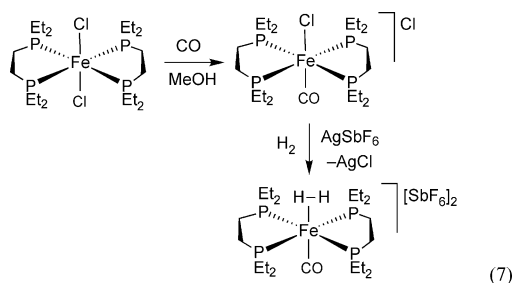
The coordination geometry of the diimine complexes is highly dependent on the donor strength of the pendant groups. Complex **1**, (N₄)FeCl₂, is an 18e octahedral species while **2**, (N₂O₂)FeCl₂, has a 5-coordinate square pyramidal structure with a dangling methoxy arm. Presumably the weaker donating ability of methoxy versus amine is responsible for the structural difference since steric factors should be minor. Although **2** is formally a 16e species, it does not readily take on sixth ligands, even CO, choosing instead to remain a high-spin complex wherein the potentially π-donating chlorides may help stabilize the electronic unsaturation.

The inability of CO to observably bind to coordinatively unsaturated Fe^{II} fragments formed e.g. upon removal of a chloride ligand from **1** and **2** is the central theme for discussion here. It should be reiterated that DuBois found that *trans*-FeCl₂(PNP)(dmpm), which is also high spin, does add CO on chloride removal.¹¹ As further background, very few paramagnetic metal–carbonyl complexes are known, and addition of CO to a high-spin complex without a subsequent spin state change is even more scarce.¹⁹ Although high-spin iron–*heme* systems readily undergo spin-crossover carbo-

(18) (a) Mezzetti, A.; Del Zotto, A.; Rigo, P.; Pahor, N. B. *J. Chem. Soc., Dalton Trans.* **1989**, 1045. (b) Chin, B.; Lough, A. J.; Morris, R. H.; Schweitzer, C.; D’Agostino, C. *Inorg. Chem.* **1994**, *33*, 6278.

(19) Two recent examples are known: (a) Hu, X.; Castro-Rodriguez, I.; Meyer, K. *J. Am. Chem. Soc.* **2004**, *126*, 13464. (b) Betley, T. A.; Peters, J. C. *Inorg. Chem.* **2003**, *42*, 5074.

nylation to form the corresponding low-spin iron–carbonyl complex,⁵ as will be shown below there are very few examples of *non-heme* high-spin Fe(II) complexes that react with and bind CO under ambient conditions. In contrast there are many low-spin Fe(II) complexes, particularly phosphine complexes, that readily react with and strongly bind CO, as exemplified by eq 7.¹³ Here chloride is easily substituted by



CO^{13a} (one Cl goes outer sphere with no need for silver salt abstraction) in stark contrast to the directly analogous Fe–diimine system (eq 1). It is interesting to note that, unlike diamagnetic *trans*-FeCl₂(depe)₂ in eq 7 and most other FeCl₂P₄ complexes, DuBois's *trans*-FeCl₂(PNP)(dmpm) complex (and a select few others²⁰) are *paramagnetic*,¹⁰ demonstrating how sensitive the spin state is to minor ligand variation, particularly steric effects.

If we get back to eq 7, Morris later found that H₂ could readily be coordinated *trans* to CO by treatment with silver salts.^{13b} The ligands are all strongly or at least moderately strongly bound, including H₂ in the dicationic species that we had hoped to mimic using the N₄ ligand set instead of diphosphines. Neither SbF₆ nor triflate counteranions tend to bind to the iron centers in these types of systems in contrast to the diimine complexes **4** and **5**. Triflate anion can displace H₂ in [Fe(CO)(H₂)(depe)₂]²⁺ but not in the more electron-poor Ph₂PC₂H₄PPh₂ (dppe) analogue; i.e., [Fe(CO)(H₂)(dppe)₂][OTf]₂ is stable (cf. **4** where OTf is tightly bound and cannot be displaced by CO).^{13b}

Thus, unlike the low-spin diphosphine system in eq 7 or DuBois's finding¹¹ that *high-spin* Fe(PNP)(dmpm)Cl₂ does add CO to form *diamagnetic* [Fe(PNP)(dmpm)Cl(CO)]⁺, the analogous reactions of CO with the high-spin diimine complexes do not give stable CO binding. The calculations on the model complexes described above indeed show essentially no *net* binding energy (enthalpically) for addition of CO to high-spin square-pyramidal [(N₄)FeCl]⁺ to form low-spin[(N₄)FeCl(CO)]⁺ but 48 kcal/mol for addition in the totally low-spin diphosphine model system. This may best be analyzed in a reverse sense in terms of instability of a CO complex toward CO dissociation, i.e., examining removal of a neutral ligand L from a saturated (18e) complex to yield a 16-electron complex as discussed by Poli.^{6d} Unlike in the saturated precursor, the HOMO–LUMO gap (ΔE) in the less saturated complex is potentially very small. Thus, if the

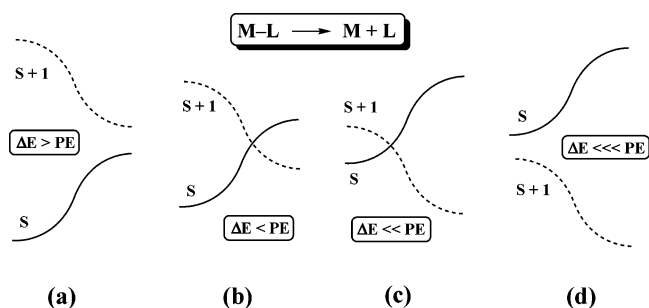


Figure 9. Possible reaction coordinates for a ligand dissociation reaction, $M-L \rightarrow M + L$ (depiction based on that in ref 6d).

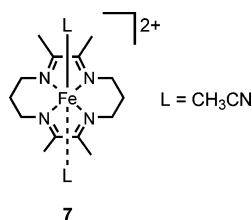
electron pairing energy exceeds ΔE , the system will prefer to adopt a spin-unpaired configuration. In general, when a coordination site (vacant orbital) is created and a metal-based lone pair is available, one may expect a spin-state dichotomy depending on the relative importance of the pairing energy (PE) and the orbital splitting (ΔE). The ligand dissociation can involve four distinct cases (Figure 9). In case a, the product generated by ligand dissociation is more stable in the same low-spin configuration as the starting complex ($\Delta E > PE$), thus any spin-related considerations can be neglected in a thermally induced reaction. This is the case for the diphosphine complexes where ΔE is dominant because of the high ligand field strength of the phosphines. In case b, the pairing energy is greater ($\Delta E < PE$), leading the unsaturated product to prefer a higher spin configuration. Thus, the product is stabilized by *unpairing* two electrons and this type of energetic stabilization of open-shell structures can be ascribed to the release of pairing energy. This concept was used to rationalize the “unusually weak” M–CO bonds in Cp₂VI(CO)^{6a} and in Cp₂Cr(CO).^{6b} If this energetic gain is larger than the necessary energy to break the bond along the starting spin state surface, situation c results ($\Delta E \ll PE$). In this case, the system is stable with a less saturated configuration because it would cost more energy to pair two electrons (thereby creating the necessary vacant orbital for the new bond) than the energetic gain resulting from the bond formation in the lower spin state. In the extreme case d, the system always remains in the higher spin state. Cases b and c are particularly interesting because they involve a change of spin state along the reaction coordinate (spin crossover reactivity), which has far-reaching implications in organometallic chemistry and catalytic processes that depend on the availability of open coordination sites.

Where the Fe–diimine system fits in the above discussion, i.e., cases b, c, or d, is not clear since the spin state of the presumably unstable CO adduct (if one forms at all) could not be determined experimentally. Case b is the least likely since a CO adduct was not actually observed and the calculations indicate CO binding would be endergonic. Case c would seem to fit, although since none of the diimine complexes synthesized were low spin (even those with bound anions), case d is possible also; i.e., the CO adduct could be a high-spin species ($S = 1$ or 2). The DFT calculations indicate that the ground state for the [*trans*-(N₄)FeCl(CO)]⁺ model is a singlet but the triplet state lies only 4.5 kcal/mol above it (versus 22.2 kcal/mol for the quintet state). For the

(20) A singlet–quintet temperature-dependent equilibrium even exists in FeCl₂(dppen)₂ (dppen = *cis*-1,2-bis(diphenylphosphino)ethylene): Cecconi, F.; Di Vaira, M.; Midollini, S.; Orlandini, A.; Sacconi, L. *Inorg. Chem.* **1981**, *20*, 3423. See also: Di Vaira, M.; Midollini, S.; Sacconi, L. *Inorg. Chem.* **1981**, *20*, 3430.

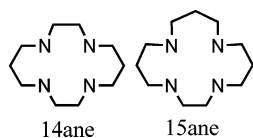
16e fragment with the CO removed, both the singlet–triplet and singlet–quintet energy gaps are much larger (18.3 and 32.1 kcal/mol, respectively), in accord with the prevalence of the quintet states for these diimine complexes. The situation is however not completely straightforward because of the critical importance of π back-bonding to the strong stability of CO coordination in stark contrast to that for hard σ donors, specifically here the anions in **4** and **5**, which have favorable binding to the hard cationic Fe centers. The calculated energy for CO binding to the $[(N_4)FeCl]^+$ model is relatively low, 30.8 kcal/mol, especially in comparison to that for the diphosphine analogue, 47.5 kcal/mol. The back-bonding ability of the diimine complexes would thus appear to be at a relatively low level because of insufficient electron richness of the metal center. Apparently the N-donor ligands are not in the same league with P-donors in this regard, although where to draw the line in any given battery of ancillary ligands may not be obvious (even more so if overall charge is also varied). In general, the electrophilicity and nucleophilicity of complexes remain surprisingly qualitative concepts in this era of sophisticated computational methodologies.

There are examples in the literature of Fe(II) diimine complexes undergoing carbonylation,²¹ but they differ in either geometry or spin state. In the first of these, the tetrahedral, paramagnetic complex $Fe(N(R)=C(H)C(H)=N(R))(I)_2$ ($R = ^iPr$) (**6**) can react with CO to form an octahedral low-spin bis adduct $6(CO)_2$.^{21a} In other examples, macrocyclic α -diimine octahedral, *low-spin* Fe^{II} dicationic complexes of the type **7** react with 1 equiv of CO to form the corresponding iron–carbonyl complex by displacement of one CH_3CN ligand.^{21b,c} Although reversible, CO binding



is at least observed in **7** at ambient temperature and 1 atmosphere of CO, unlike for our systems. Also unlike **4** and **5**, the PF_6^- anions in **7** show no proclivity to coordinate to the iron.

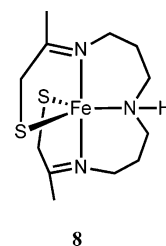
Bis(acetonitrile)iron complexes very similar to **7** but with saturated macrocyclic amines were reported by Stynes to also undergo displacement of one acetonitrile by CO.²² The 14ane



(21) (a) Breuer, J.; Fruhauf, H.-W.; Smeets, W. J. J.; Spek, A. L. *Inorg. Chim. Acta.* **1999**, *291*, 438. (b) Goedken, V. L.; Park, Y.; Peng, S.-M.; Norris, J. M. *J. Am. Chem. Soc.* **1974**, *96*, 7693. (c) Baldwin, D. A.; Pfeiffer, R. M.; Reichgott, D. W.; Rose, N. J. *J. Am. Chem. Soc.* **1973**, *95*, 5153.

complex is low-spin and the 15ane complex is high-spin, and both reversibly react with CO (1 atm) in acetonitrile to form low-spin $[Fe(ane)(CH_3CN)(CO)]^{2+}$. However, the reaction of the paramagnetic 15ane complex showed only barely visible color and spectral changes at room temperature, and low temperatures ($-30\text{ }^\circ\text{C}$) were needed for reaction completion. The 15ane complex showed a 2000-fold greater CO dissociation rate than the 14ane complex. This was ascribed to effects of ring size: both rings are too large to ideally accommodate a low-spin Fe, and the larger 15ane ring especially disfavors the low spin state. In hemoglobin the opposite is true; the ring size is more ideal for the low-spin state.

Tridentate N-donor systems are also relevant here.²³ Ellison et al. report a more recent example of a high-spin Fe^{II} complex (**8**) undergoing carbonylation at low temperature to form a metastable species that readily loses CO when the temperature is raised.^{23a} **8** undergoes distinct reversible color



changes on cooling to $0\text{ }^\circ\text{C}$ or below (indicating CO uptake) and on subsequent warming (loss of CO), and ν_{CO} was observed at 1929 cm^{-1} at $-65\text{ }^\circ\text{C}$. Our reactions of diimine complexes with CO were performed between -40 and $25\text{ }^\circ\text{C}$, and no solution color change was observed. It is possible that CO binding was occurring to a very small extent, which we were unable to detect (low-temperature IR could not be done in situ). The thiolate ligands in Ellison's *neutral* complex presumably raise the ligand field strength and the π donor ability of the metal sufficiently enough to form an observable CO adduct versus our *cationic* all N-donor system. Rauchfuss indeed later demonstrated that CO coordinated robustly to $[(Me_3TACN)FeL_n]^+$ ($Me_3TACN =$ tridentate amine; $n = 1, 2$) for strong-field $L = SPh$ (and CN) but bound only reversibly for $L = iodide$.^{23b} As found for our complexes **1** and **2**, high-spin $(Me_3TACN)FeCl_2$ totally rejected binding of CO.

In contrast to the above systems and our results, very low-coordinate high-spin iron complexes have recently been found to readily undergo spin crossover on CO addition (case b or c). Thus, 3-coordinate $(nacnac)FeR$ ²⁴ ($nacnac =$ bulky β -diketiminate) and 4-coordinate $[PhB(CH_2P^iPr_2)_3]FeCl$ ^{19b} type species bind CO readily and give a low-spin CO insertion/addition product, $(nacnac)Fe(CO)_2(COR)$, and a low-spin Fe^{II} carbonyl adduct, respectively. In the latter case the anionic chelator on the iron center is a strong-field ligand,

(22) Stynes, D. V.; Hui, Y. S.; Chew, V. *Inorg. Chem.* **1982**, *21*, 1222.

(23) (a) Ellison, J.; Nienstedt, A.; Shoner, S. C.; Barnhart, D.; Cowen, J. A.; Kovacs, J. A. *J. Am. Chem. Soc.* **1998**, *120*, 5691. (b) Moreland, A. C.; Rauchfuss, T. B. *Inorg. Chem.* **2000**, *39*, 3029.

(24) Smith, J. M.; Lachicotte, R. J.; Holland, P. L. *Organometallics* **2002**, *21*, 4808.

which can facilitate spin crossover. In the former case, addition of *multiple* CO to the highly unsaturated complex not surprisingly results in a low-spin system. These results once again demonstrate that the effects of spin state are very dependent on factors such as ligand field strength, and overall coordination geometry and charge.

Conclusions

There is a surprisingly large range in reactivity toward CO for the Fe^{II} complexes discussed in this paper. Some fragments bind CO very strongly such as [FeCl(depe)₂]⁺, others reversibly, and our diimine complexes not at all. The latter high-spin iron^{II} centers containing multidentate N- or N,O-donor ligands prefer to bind weakly coordinating anions such as SbF₆⁻ and OTf⁻ rather than undergo spin crossover and bind strongly π -accepting CO. The preference to interact with the hard-donor anions illustrates the unexpectedly high electrophilic nature of these complexes and suggests description of the Fe^{II} centers here as “hard acids”. Although CO has a well-established ability to bind to highly electrophilic cationic complexes, including homoleptic species such as [Fe(CO)₆]²⁺,²⁵ it is notable that CO does not coordinate to the cationic Fe–diimine systems. This indicates that the Fe center here would be a poor π donor to CO in a low-spin state, but it is not intuitively obvious that the imine/amine or imine/methoxy ligands would render the Fe that electron poor. This notion along with calculations showing that addition of CO to a high-spin Fe–diimine model complex is essentially thermoneutral suggest that these and related reactions discussed above are strongly influenced by spin effects.^{6,12} The ligand field strengths are critical: the diimine complexes do not bind CO even weakly, but as expected, analogues containing diphosphines with strong ligand fields bind CO tightly, even in dicationic species with potentially coordinating anions such as triflate. Calculations as described here are thus useful in understanding and predicting whether spin crossover on ligand addition is disfavored thermodynamically or kinetically (e.g. a “spin block” effect¹²).

Last, it may seem ironic that binding of CO to hemoglobin is one of the few facile “spin-forbidden” reactions of this toxic molecule with Fe^{II} centers. On the other hand, Nature has designed hydrogenase enzymes to possess low-spin Fe centers that powerfully and purposefully bind CO. Hydrogenases must possess enough electron density at iron to strongly bind CO while maintaining a fine balance of electrophilic character to reversibly bind and heterolytically cleave H₂. The peculiar presence in these enzymes of *cyanide* ligands, which significantly can be formed biologically along with CO,^{7b} could be related to their high ligand-field strength (much like abiological phosphines). This would assist in maintaining a low-spin configuration for Fe throughout the large known array of redox state and ligation changes^{7c,e–g} that occur during the function of the enzyme.

Labiality of either CO or CN would be deadly here. Weaker field ligand sets than CO/CN such as those typically found in enzymes (histidine, cysteine, etc.) would not fulfill this function since, as can be seen here, tetradentate N-donor ligand sets such as imine/amine (or tridentate amine^{23b}) give *high-spin* complexes incapable of even weak CO binding. In this context Rauchfuss had previously also demonstrated the positive influence of cyanide on binding of CO to Fe^{II} and on facilitating carbonylation of Fe^{II} thiolate complexes.^{23b,26}

Experimental Section

All manipulations and reactions were performed either under a helium atmosphere in a Vacuum Atmospheres drybox or under argon or CO atmospheres using standard Schlenk techniques unless otherwise specified. Toluene, tetrahydrofuran (THF), MeOH, and CDCl₃ were dried and degassed prior to use. All CO reactions were performed between –40 and 25 °C. FeCl₂, AgSO₃CF₃, and AgSbF₆ were purchased from Acros and used as received. NaBAR^f and N₄, N₂O₂, and N₂S₂ ligands were prepared according to literature procedures¹⁰ or as below. ¹H NMR were recorded on a Bruker 400 MHz spectrometer, and all shifts were referenced to a capillary of CDCl₃. μ_{eff} was determined through the use of Evan’s method with CDCl₃ as the solvent in the NMR tube and the capillary.

Alternate Syntheses of Diimine Ligands. A slight variation of the general literature procedure previously reported¹⁰ for the syntheses of the N₄, N₂O₂, and N₂S₂ ligands is given here and gave better results for the N₄ ligand in particular. For preparation of N₄, *N,N*-dimethylaminopropylamine (22 g, 0.2 mmol) was added to 2,3-butanedione (8.61 g, 0.1 mmol) in 300 mL of ethanol. The reaction mixture was refluxed for 5 h. The resulting dark brown/black mixture was then dried with MgSO₄ and distilled under high vacuum to yield 12–15 g (ca. 50% yield) of the N₄ ligand as a tan viscous liquid. The latter will darken when exposed to the atmosphere and should be protected from air. The N₂O₂ and N₂S₂ ligands were prepared analogously from 3-methoxypropylamine and 2’-(2-thienyl)ethylamine, respectively.

Synthesis of N₄FeCl₂ (1). To a solution of FeCl₂ (1.27 g, 10 mmol) in THF (30 mL) was slowly added the N₄ ligand (2.54 g, 10 mmol). Upon stirring at RT (room temperature) the solution slowly takes on a dark blue color overnight, indicating formation of the N₄FeCl₂ product. Volatiles were removed in vacuo leaving a dark ink-blue solid. Yield: 3.42 g, 90%. μ_{eff} : 5.03 μ_{B} (0.052 M solution). ¹H{¹³C} NMR: δ –44.9, 4.4, 6.3, 13.1, 52.1, 85.5. Anal. Calcd for C₁₄H₃₀Cl₂N₄Fe: C, 44.12; H, 7.93; N, 14.70. Found: C, 44.40; H, 8.07; N, 14.30.

Synthesis of (η^3 -N₂O₂)FeCl₂ (2). The same procedure as above was used for reaction of 1.27 g of FeCl₂ and 2.28 g of N₂O₂ in 30 mL of THF. Color change occurred overnight to a dark blue indicating the formation of **2**. Yield: 3.28 g, 92%. μ_{eff} : 4.87 μ_{B} (0.031 M solution). ¹H{¹³C} NMR: δ –7.2, 1.4, 8.6, 18.3, 32.6, 49.2, 80.7. Anal. Calcd for C₁₂H₂₄Cl₂N₂O₂Fe: C, 40.59; H, 6.81; N, 7.89. Found: C, 40.59; H, 6.88; N, 7.52.

N₂S₂FeCl₂ (3). The same procedure was used as for synthesis of N₄FeCl₂. A 1.27 g (10 mmol) amount of FeCl₂ and 2.44 g (10 mmol) of N₂S₂ were added together in 30 mL of THF. Upon being stirred overnight, the solution took on a deep blue color. After removal of volatiles, a dark blue solid was isolated. Yield: 3.13 g, 84%. μ_{eff} : 4.75 μ_{B} (0.096 M solution). ¹H{¹³C} NMR: δ –6.6,

(25) (a) Aubke, F.; Wang, C. *Coord. Chem. Rev.* **1994**, *94*, 483. (b) Xu, Q. *Coord. Chem. Rev.* **2002**, *231*, 83. (c) Finze, M.; Bernhardt, E.; Willner, H.; Lehmann, C. W.; Aubke, F. *Inorg. Chem.* **2005**, *44*, 4206.

(26) Rauchfuss, T. B.; Contakes, S. M.; Hsu, S. C. N.; Reynolds, M. A.; Wilson, S. R. *J. Am. Chem. Soc.* **2001**, *123*, 6933.

Table 4. Crystal and Structure Refinement Data for **1**

empirical formula	C ₁₆ H ₃₂ Cl ₈ FeN ₄
fw	619.91
color	dark blue
temp	203(2) K
cryst system	monoclinic
space group	C2/c
unit cell dimens	<i>a</i> = 16.3145(13) Å <i>b</i> = 9.2831(8) Å <i>c</i> = 19.4183(17) Å β = 112.162(2)°
<i>V</i>	2723.6(4) Å ³
<i>Z</i>	4
θ range for data collcn	2.26–22.83°
index ranges	−17 ≤ <i>h</i> ≤ 17, −9 ≤ <i>k</i> ≤ 9, −19 ≤ <i>l</i> ≤ 20
reflcs collcd	4347
indpndt reflns	1755 [R(int) = 0.0288]
data/restraints/params	1755/0/132
goodness-of-fit on <i>F</i> ²	1.299
final R indices [<i>I</i> > 2σ(<i>I</i>)]	R1 = 0.0369, wR2 = 0.0898
R indices (all data)	R1 = 0.0463, wR2 = 0.0930

6.3, 9.4, 11.2, 50.6, 63.0, 111.0. Anal. Calcd for C₁₂H₂₄Cl₂N₂S₂Fe: C, 37.23; H, 6.25; N, 7.23. Found: C, 37.35; H, 6.26; N, 7.01.

N₄Fe(OTf)₂ (4). Attempted syntheses of [(N₄)Fe(CO)(Cl)][OTf] resulted in the isolation of N₄Fe(OTf)₂. Following the same general procedures listed above and even when 0.8 equiv of AgOTf was used, the only isolated product was a purple crystalline material of composition N₄Fe(OTf)₂ in poor yields (10–15%). The complex was prepared and isolated in good yield when 2 equiv of AgOTf (0.262 g, 2 mmol) was added to the N₄FeCl₂ (0.191 g, 1 mmol) in cold (0 °C) toluene (20 mL). The solution was then stirred overnight followed by subsequent filtration. The supernatant was stored at −40 °C for 1 week whereupon dark red/purple crystals of **4** formed. Yield: 0.216 g, 61%. NMR indicated a paramagnetic compound, but μ_{eff} was not determined.

[(η^3 -N₂O₂)Fe(μ -Cl)(SbF₆)₂] (5). AgSbF₆ (1.72 g, 5 mmol) was slowly added to a cold (−40 °C) CO-saturated solution of toluene (20 mL) containing 1.77 g (5 mmol) of N₂O₂FeCl₂ [NOTE: CO is not necessary for the synthesis]. Within 30 min a white precipitate was observed. The solution was allowed to continue to stir for 4 h and then stored at −40 °C under CO atmosphere overnight. The solution was then filtered at room temperature and the supernatant pumped in vacuo to incipient crystallization (10 mL) followed by cooling to −40 °C, whereupon large dark red/purple crystals of **5** formed over the course of 2 d. No CO stretch indicative of CO binding was observed in the final product. Yield: 2.14 g, 77%. μ_{eff} : 4.84 μ_{B} (0.024 M solution). ¹H{¹³C} NMR: δ −6.2, 2.3, 4.5, 8.2, 55.4, 67.3, 71.9.

Crystal Structure Determinations. The crystal structures of **1**, **2**, **4**, and **5** were determined as follows, with exceptions noted in subsequent paragraphs. Crystal data are given in Tables 4–7. In all cases, a crystal was mounted onto a glass fiber using a spot of silicone grease. Due to air sensitivity, the crystal was mounted from a pool of mineral oil under argon gas flow. The crystal was placed on a Bruker P4/CCD diffractometer and cooled to 203 K using a Bruker LT-2 temperature device. The instrument was equipped with a sealed, graphite-monochromatized Mo K α X-ray source (λ = 0.710 73 Å). A hemisphere of data was collected using ϕ scans, with 30-s frame exposures and 0.3° frame widths. Data collection and initial indexing and cell refinement were handled using SMART²⁷ software. Frame integration, including Lorentz–polarization corrections, and final cell parameter calculations were carried out using SAINT²⁸ software. The data were corrected for absorption

(27) SMART-NT 4; Bruker AXS, Inc.: Madison, WI 53719, 1996.

(28) SAINT-NT 5.050; Bruker AXS, Inc.: Madison, WI 53719, 1998.

Table 5. Crystal and Structure Refinement Data for **2**

empirical formula	C ₁₂ H ₂₄ Cl ₂ FeN ₂ O ₂
fw	355.08
color	dark blue
temp	203(2) K
cryst system	triclinic
space group	P $\bar{1}$
unit cell dimens	<i>a</i> = 10.6055(7) Å <i>b</i> = 10.6869(7) Å <i>c</i> = 14.5662(9) Å α = 87.532(1)° β = 89.140(1)° γ = 86.070(1)°
<i>V</i>	1645.40(18) Å ³
<i>Z</i>	4
θ range for data collcn	1.91–28.47°
index ranges	−13 ≤ <i>h</i> ≤ 13, −14 ≤ <i>k</i> ≤ 14, −18 ≤ <i>l</i> ≤ 19
reflcs collcd	11 142
indpndt reflns	6466 [R(int) = 0.0337]
data/restraints/params	6466/0/343
goodness-of-fit on <i>F</i> ²	1.130
final R indices [<i>I</i> > 2σ(<i>I</i>)]	R1 = 0.0578, wR2 = 0.1092
R indices (all data)	R1 = 0.0945, wR2 = 0.1214

Table 6. Crystal and Structure Refinement Data for **4**

empirical formula	C ₁₆ H ₃₀ F ₆ FeN ₄ O ₆ S ₂
fw	608.41
color	dark purple
temp	203(2) K
cryst system	monoclinic
space group	P2 ₁ / <i>n</i>
unit cell dimens	<i>a</i> = 10.957(7) Å <i>b</i> = 16.085(8) Å <i>c</i> = 14.554(9) Å β = 92.345(7)°
<i>V</i>	2563(3) Å ³
<i>Z</i>	4
θ range for data collcn	1.89–23.22°
index ranges	−12 ≤ <i>h</i> ≤ 11, −16 ≤ <i>k</i> ≤ 8, −16 ≤ <i>l</i> ≤ 16
reflcs collcd	7897
indpndt reflns	3257 [R(int) = 0.0259]
data/restraints/params	3257/0/340
goodness-of-fit on <i>F</i> ²	1.408
final R indices [<i>I</i> > 2σ(<i>I</i>)]	R1 = 0.0709, wR2 = 0.2256
R indices (all data)	R1 = 0.0807, wR2 = 0.2343

Table 7. Crystal and Structure Refinement Data for **5**

empirical formula	C ₂₄ H ₄₈ Cl ₂ F ₁₂ Fe ₂ N ₄ O ₄ Sb ₂
fw	1110.74
color	dark purple
temp	203(2) K
cryst system	monoclinic
space group	P2 ₁ / <i>c</i>
unit cell dimens	<i>a</i> = 10.243(3) Å <i>b</i> = 12.995(4) Å <i>c</i> = 14.809(5) Å β = 97.150(7)°
<i>V</i>	1955.7(11) Å ³
<i>Z</i>	2
θ range for data collcn	2.00–25.38°
index ranges	−12 ≤ <i>h</i> ≤ 12, −15 ≤ <i>k</i> ≤ 13, −17 ≤ <i>l</i> ≤ 17
reflcs collcd	12 434
indpndt reflns	3589 [R(int) = 0.0872]
completeness to θ = 25.38°	99.9%
goodness-of-fit on <i>F</i> ²	1.159
final R indices [<i>I</i> > 2σ(<i>I</i>)]	R1 = 0.0836, wR2 = 0.1319
R indices (all data)	R1 = 0.1236, wR2 = 0.1434

using the SADABS²⁹ program. Decay of reflection intensity was monitored via analysis of redundant frames. The structure was solved using direct methods and difference Fourier techniques. All

(29) Sheldrick, G. SADABS, first release; University of Göttingen: Göttingen, Germany.

hydrogen atom positions were idealized and rode on the atom they were attached to. The final refinement included anisotropic temperature factors on all non-hydrogen atoms. Structure solution, refinement, graphics, and creation of publication materials were performed using SHELXTL NT.³⁰ Additional details of data collection and structure refinement are listed in Table 1. For the structure of **4**, the disordered triflate ligands were refined in two disordered positions. The disordered sulfur atom positions and site occupancy factors (SOF) were refined along with their SOF's tied to 1.0. This resulted in site occupancy factors of 0.80(2) and 0.20(2) for S2 and S2A, respectively, and 0.84(1) and 0.16(1) for S1 and S1A, respectively. In addition, the oxygen atom positions O5

and O6 were each refined in two positions, with site occupancy factors set at 0.75 and 0.25 for the two positions (O5/O5A and O6/O6A).

Acknowledgment. This research was supported by the Department of Energy, Office of Science, Office of Basic Energy Sciences, Chemical Sciences Division. We are grateful to Ken Caulton for helpful discussions regarding this work.

Supporting Information Available: Crystallographic data for **1**, **2**, **4**, and **5** in CIF format and a complete list of authors in refs 5a and 17. This material is available free of charge via the Internet at <http://pubs.acs.org>.

IC050966H

(30) SHELXTL NT, version 5.10; Bruker AXS, Inc.: Madison, WI 53719, 1997.